

PAPER

CrossMark
click for updatesCite this: *RSC Adv.*, 2015, 5, 50512

Rapid detection of *Fusarium* wilt in basil (*Ocimum* sp.) leaves by desorption electrospray ionization mass spectrometry (DESI MS) imaging†

R. G. Hemalatha,^a Hemanta R. Naik,^a Vasundhara Mariappa^b and T. Pradeep^{*a}

Basil (*Ocimum* sp.), a medicinal herb is used fresh and/or dry in various (culinary, cosmetic and pharmaceutical) preparations. *Fusarium* wilt caused by the fungus *Fusarium oxysporum* f. sp. *basilici* is limiting basil cultivation in many countries. Since the leaf is the edible part in basil, new approaches are required to identify, and to prevent the spread of *Fusarium* pathogens. Desorption electrospray ionization mass spectrometry (DESI MS) was used for imaging thin layer chromatography (TLC) – imprints of leaves of three different species of basil (*Ocimum basilicum* L., *O. tenuiflorum* L., and *O. gratissimum* L.), and the molecular manifestations during *Fusarium* contamination are recorded. DESI MS images showed the chemotaxonomic differences of basil species and the changes in metabolite ion peaks during pathogen infection. Besides easy detection of reported toxic metabolite(s) of the pathogen(s), the results include molecular images showing spatial distribution of all coexisting surface-bound metabolites in plant leaves, their fragment ions, and the transient changes in their spatial distribution during *Fusarium* attack under natural conditions. Demonstration of the same protocol to image seedling, young/mature leaves, basil/other related plant (Patchouli – *Pogostemon cablin* (Blanco) Benth.), wilt/other disease symptoms shows that prior knowledge of the metabolite profile of the plant/pathogen is not required. This rapid detection method can be tailored to large scale screening programs for plant diseases suggesting potential implications in agriculture and quarantine requirements.

Received 19th December 2014
Accepted 20th May 2015

DOI: 10.1039/c4ra16706f

www.rsc.org/advances

Introduction

Mass spectrometry in natural product research is unraveling several unprecedented possibilities. From the traditional chemical ionization to the recent ambient ionization, various methods are available to analyze diverse classes of natural compounds.¹ With the advent of desorption electrospray ionization mass spectrometry, the capability of doing ionization outside the mass spectrometer under ambient/native conditions is largely exploited for developing various ambient ionization techniques.² While direct ambient ionization of intact plant material is demonstrated, certain ambient ionization methods like imprint imaging gives the spatial distribution of compounds in two or three dimensional space.³ Imaging mass spectrometry including desorption electrospray mass spectrometry (DESI MS) has been used to study microbes in cultures,^{4,5} but it is necessary to identify disease causing

pathogens in intact plant tissues to isolate contaminated planting materials, especially, in emergencies of disease epidemics like *Fusarium* wilt. The genus *Fusarium* includes several pathogenic fungal species,⁶ whose outbreak has caused huge economic loss in many crops. In this study, we demonstrate the rapid detection of *Fusarium* wilt contamination in leaves of different basil species by DESI MS imaging.

Basil (*Ocimum* sp.) is a traditional, revered home-grown plant with long history of use and cultivation in India. The commercial success of sweet basil (*Ocimum basilicum* L.) as a culinary herb is evident from its widespread use in various popular cuisines. Its quick growing habit and suitability for different climatic conditions has promoted its large scale cultivation, worldwide.⁷ A number of domestic cultivars, breeding lines and hybrids are available with variety of unique aromas/tastes (like clove, citrus, camphor, cinnamon, licorice, etc.) giving them special market price and export quality.⁸ Essential oils, polyphenols, flavonoids and other bioactive molecules in them are commercially exploited as flavoring agents and in perfumes, cosmetics and pharmaceutical preparations.

Fusarium wilt is a production constraint in basil and its occurrence is reported from different parts of the world.⁹ The disease is caused by *Fusarium oxysporum* f. sp. *basilica* (Fob). It is one among the 120 host-specific, individual strains (formae species) of the wilt pathogen, *Fusarium oxysporum* (Fox).¹⁰ The

^aDST Unit on Nanoscience and Thematic Unit of Excellence, Department of Chemistry, Indian Institute of Technology Madras, Chennai, India. E-mail: pradeep@iitm.ac.in; Fax: +91-44-2257-0509; +91-44-2257-0545; Tel: +91-44-22574208

^bMedicinal and Aromatic Section, Department of Horticulture, University of Agricultural Sciences, Bangalore, India

† Electronic supplementary information (ESI) available. See DOI: 10.1039/c4ra16706f

presence of *Fusarium* pathogenic fungal species complex in the common environment causes diseases (like keratitis, fusariosis etc.), in human and animals.^{11,12} The pathogenic species is identified by polymerase chain reaction (PCR) and other molecular methods.¹³ *Fusarium* remains dormant in soil for decades and comes to life on finding a suitable host. The symptomless infection present in plant parts spread through planting materials, irrigation water, farm tools, drainages, etc. The control measures taken up with chemical pesticides and sterilization of soil are inefficient. Resistance to *Fusarium* wilt is searched in accessions of *Ocimum* species and resistant basil varieties have been developed.^{14,15} Planting resistant varieties have also been challenged by new pathogenic races of *Fusarium*, which has resulted in recurrence of *Fusarium* epidemics in several crops including banana and cereals.¹⁶ Besides, aerial dissemination of the pathogens through the infected basil foliage is a major concern.¹⁷ Exceptionally low level of inoculum found in healthy leaves and seeds would introduce the pathogen into a new host or new geographical area. The major concern is that market demand for fresh, green basil leaves remains high; every day tons of basil leaves are transported and used fresh or dry, or extracted/macerated to enhance the flavor of herbal teas, food ingredients and oil.¹⁸ The changes reflected in the preparations, made from infected basil leaves remain elusive. Also, the effect of Fob on human health is not known. Hence, in this study, mass spectrometry based imaging method is demonstrated for rapid detection of *Fusarium* contamination in basil leaves under ambient conditions. Here three different aspects were addressed: the chemotaxonomic differences among three different basil species (*Ocimum basilicum* L., *O. tenuiflorum* L. and *O. gratissimum* L.) grown in natural conditions were unraveled, by imaging the TLC-imprints of their leaves using DESI MS. Likewise, *Fusarium* contaminated leaves were imaged under ambient conditions to delineate them from the healthy ones in all selected basil species. The suitability of the method in screening other related plant/disease is illustrated with Patchouli (*Pogostemon cablin*).

Experimental

Plant material

Two basil species, namely, *O. basilicum* L. and *O. tenuiflorum* L. (syn. *O. sanctum* L.) growing under natural conditions in the Indian Institute of Technology Madras (IITM) campus were used for the study. Young seedlings of Clove basil (*O. gratissimum* L.) and Patchouli (*Pogostemon cablin* (Blanco) Benth.) collected from University of Agricultural Sciences (UAS) campus, Bangalore were grown in a nursery at IITM campus. The study period was from March 2012 to October 2014.

Scanning electron microscopy

The morphology of the lower side of the healthy and *Fusarium* wilt infected leaf of basil and patchouli were observed by scanning electron microscopy (SEM) (FEI QUANTA-200). A small portion of the leaf with and without wilt symptom was fixed on the top of aluminium stub using double sided carbon tape. In

order to minimize the charging effect, SEM measurements were done using the environmental mode with a large field detector.

DESI MS imaging

A Thermo-Fisher Scientific LTQ ion trap mass spectrometer equipped with a DESI ion source was used for the study. Two TLC plates were cut in proportion to the size of the selected, detached leaf; with the leaf placed in between and sandwiched with tissue papers, TLC-imprints were made by applying a pressure of 1–4 tons for 5–10 s. Further details on the method of TLC-imprinting and the chemicals required for imaging are explained in our previous report.¹⁹ DESI MS images were acquired by continuously moving the surface beneath the spray at a constant speed, over the whole TLC-imprinted surface on a row-by-row basis (as shown in TOC graphic). The pixel size (250 × 250 μm) was determined by the total scan time of the mass spectra and the x–y scanner speed. Two operation modes (both negative and positive) and a mass range of *m/z* 50–2000 was used for imaging. Three different solvents (methanol, acetonitrile and chloroform) were used for optimization of the protocol. Elaborate details on processing and interpretation of acquired data with spectrum search tool of online databases were given in our previous report.¹⁹ For this study, the acquired data was also processed using MZmine, open-source software.²⁰

Results and discussion

The antibacterial and antifungal activities of *Ocimum* sp. are well known,²¹ but its susceptibility to *Fusarium* wilt has to be understood in detail to prevent outbreak of the disease. To check the reactions of resistance/susceptibility, in this study, three species of basil and patchouli were grown outdoors at IIT campus, in the same soil next to each other. No known chemical control was applied for *Fusarium* wilt, and resistant varieties were not planted. The selected plant species were grown under natural conditions, with no external application of manures, chemical fungicides or bio-control agents. Though commercial kits are developed for molecular identification of types of *Fusarium* pathogen present in the soil, they require technical knowledge.²² Therefore, customized methods suitable for rapid detection of contaminated leaves within hours is focused for this study. Here, the predominant metabolite ion peaks present on the leaves of healthy *versus* infected ones were compared and the contaminated ones were rapidly identified. To understand the metabolic state of the plant at any given time of pathogen infection, the spatial distribution of untargeted metabolite profile in a healthy leaf for a select mass range was used as base information to identify the infected/contaminated leaves.

The predominant metabolite profile of the selected basil species and patchouli were recorded using TLC-imprints of fresh leaves, as explained in our previous report,¹⁹ Both positive and negative ionization mode data were collected for each species. As the data acquired are voluminous, the peaks that eluted using methanol as spray solvent in the mass range of *m/z* 50–1000 from positive ionization mode alone are given in this manuscript. Fig. 1A and B and 2A–E show the DESI MS spectra

and images for spatial distribution of predominant metabolites of healthy leaf in control plants of all selected species. Illustrations given here show the similarities and variations in metabolite profile within a single leaf (*O. basilicum*-Fig. 1A and B), between young and mature leaf of same species-*O. gratissimum* (Fig. 2C and D), variations within *Ocimum* genus (Fig. 1A, B and 2A–D) and between genus (*Ocimum* and *Pogostemon*-Fig. 1A, 2A–C and E).

It is possible to identify the similarities and differences of the upper and lower leaf surfaces of a single leaf by imaging their TLC-imprints separately. Insets in Fig. 1A(a and b) show the TLC-imprints of upper and lower surfaces, respectively of a single leaf of *O. basilicum*. The corresponding DESI MS images in insets (c and d) of Fig. 1A show the faithful reproduction of TLC-imprints of the upper and lower surfaces as molecular images. As shown in Fig. 1B, the TLC-imprint of the upper leaf surface does not contain any venation pattern; but, on imaging that imprint, vein like spatial distribution was observed in DESI MS images for the metabolite ions m/z 201 and m/z 365 whereas for the ion m/z 797 (Fig. 1B) was exactly similar to the imprint as shown in Fig. 1B; this is an illustration to show that these molecular images are not artifacts. Moreover, it is possible to identify some new information by DESI MS which are not detected by conventional measurements using extracts. An example is the finer molecular detail present on the leaf margin as shown in DESI MS images for m/z 405, m/z 489 in Fig. 1B. Leaf margin (Fig. S1A†) is one of the diagnostic leaf characteristics to categorize some plant species including basil by the morphological features;^{23a} so far molecular methods are used to distinguish physical similarities.^{23b}

The leaves of *O. tenuiflorum* and *O. basilicum* look similar and have to be differentiated based on the colors of their inflorescences (Fig. S1B†). The advantage of DESI MS imaging is that the molecular differences can be identified at any stage of plant growth, without waiting for the flowering stage; here the molecular similarities and differences were understood by comparing the predominant peaks of both species of *O. tenuiflorum* and *O. basilicum* (Fig. 1A and 2A). There were overlaps found in metabolite ions for several major (m/z 201 and m/z 378) and minor peaks (m/z 104, 197, 365, 797, etc.). *De novo* sequencing and transcriptomics information available for *O. basilicum* and *O. tenuiflorum* confirms the presence of transcripts responsible for such similarities and differences in the metabolite profiles.²⁴ In this study, the characteristic predominant peaks for each species of basil are unique (for example m/z 349 for *O. gratissimum*, m/z 378 for *O. tenuiflorum* and m/z 201 for *O. basilicum*), which were used as markers to identify each basil species in further experiments. The reproducibility of these results was confirmed using samples collected from other growing areas for all selected species. It is interesting to note that samples picked from a local market also showed a similar spatial distribution of metabolites; an example is shown in Fig. S2,† wherein the spatial distribution of m/z 104, m/z 197, m/z 797 are similar to those given in Fig. 1A and B. Hence, besides identifying similarities, the predominant peak(s) may be used as unique molecular signatures/metabolite markers in plant species identification.

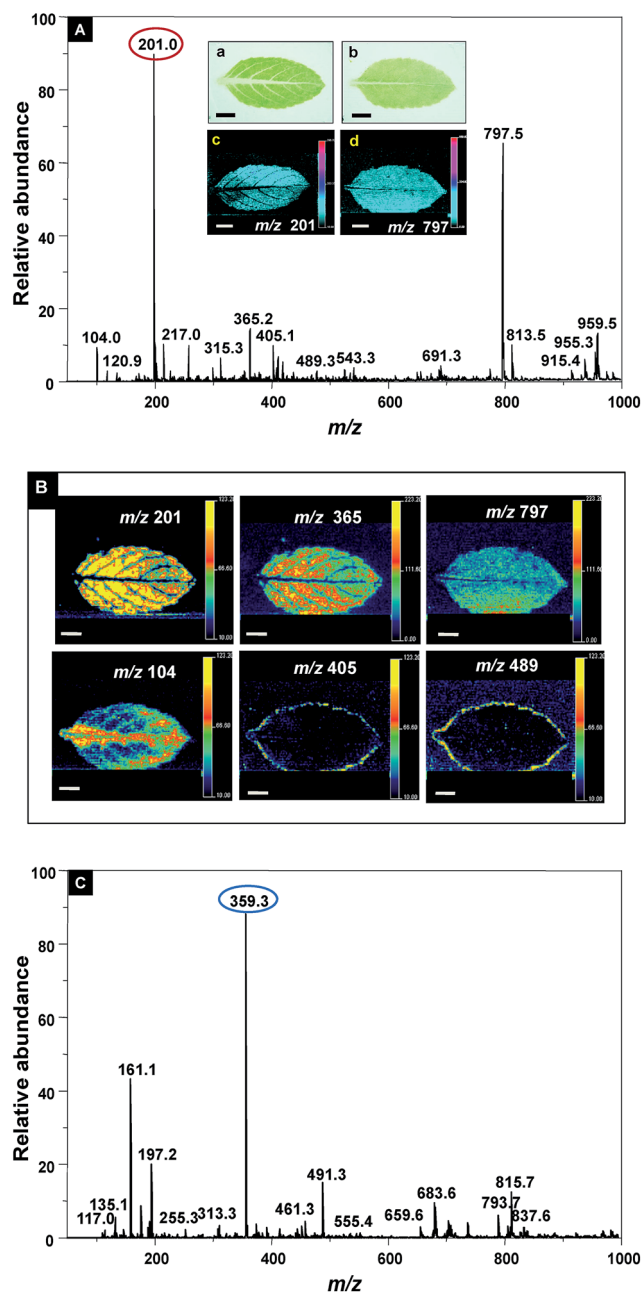


Fig. 1 DESI MS spectrum (A) and images (B) showing the predominant metabolites on the leaf of *O. basilicum*. Spectra shows the predominant metabolite peaks in positive (A) and negative (C) ionization mode, eluted in the mass range of m/z 50–1000 using methanol as spray solvent. Peak(s) which can be used for basil species identification is encircled. Insets in A shows the photographs of TLC-imprints of lower (a) and upper (b) surface of the basil leaf, and the corresponding DESI MS images for the ion m/z 201 and 797 of lower (c) and upper (d) surface are shown below. (B). Images corresponding to various ions from the upper surface of the leaf. The scale is uniform in all the images (5 mm). The major peaks where differences are seen are highlighted as DESI MS images.

Solvent plays a major role in the elution of each category of the compound.²⁵ When different solvents (methanol, acetonitrile, chloroform) were used, there were differences in metabolite profile recorded, as shown in Fig. 3A for *O. gratissimum*.

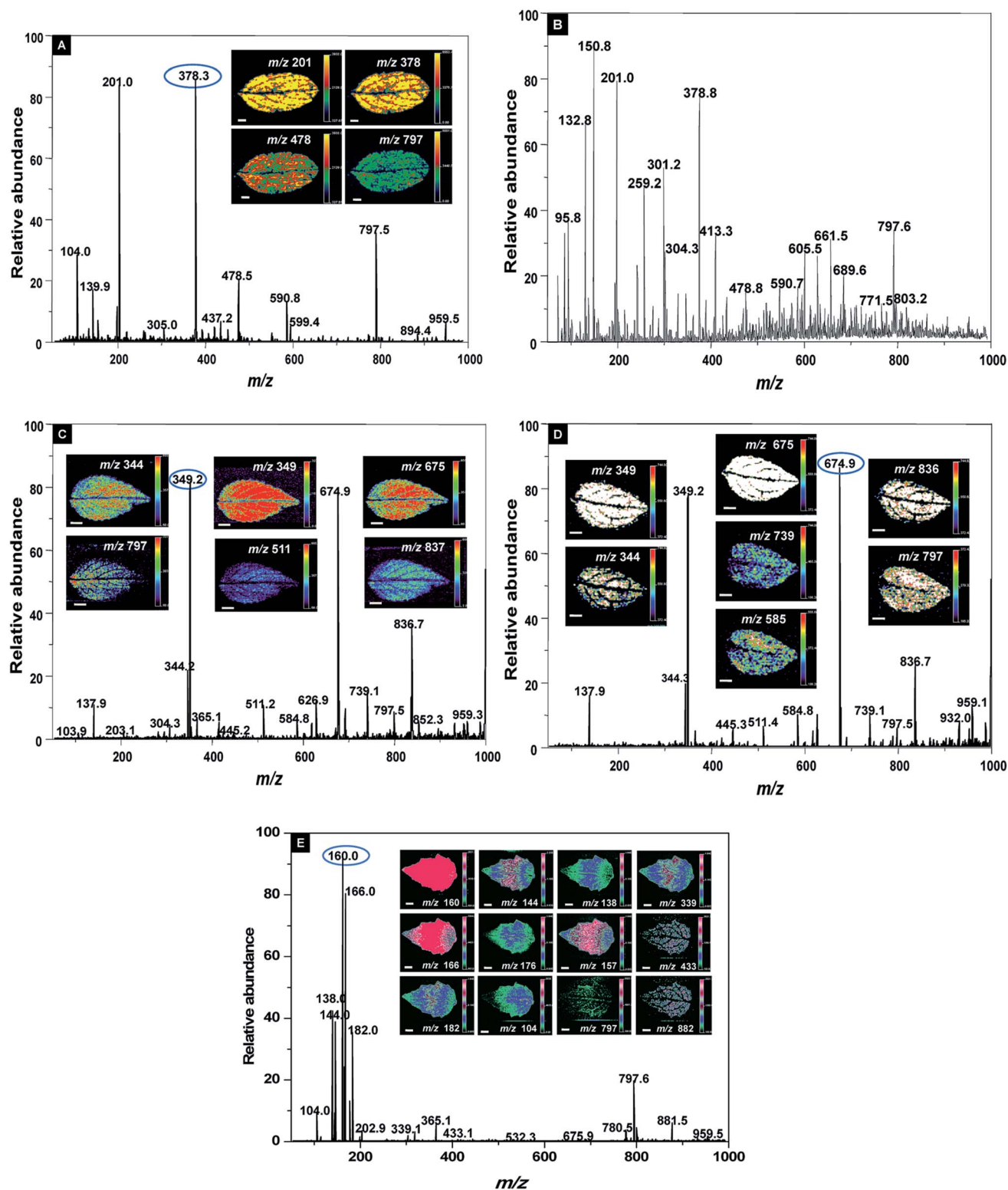


Fig. 2 DESI MS spectra and images showing the variations in predominant metabolites using (A) TLC-imprint, (B) direct detection from detached leaf of *O. tenuiflorum*. Other illustrations are showing variations between (C) mature leaf versus (D) young leaf of *O. gratissimum* and (E) *P. cablin*. The scale is uniform in all the images (5 mm). Predominant peak representing species identity is encircled. The major peaks where differences in spatial distribution are seen are highlighted as DESI MS images.

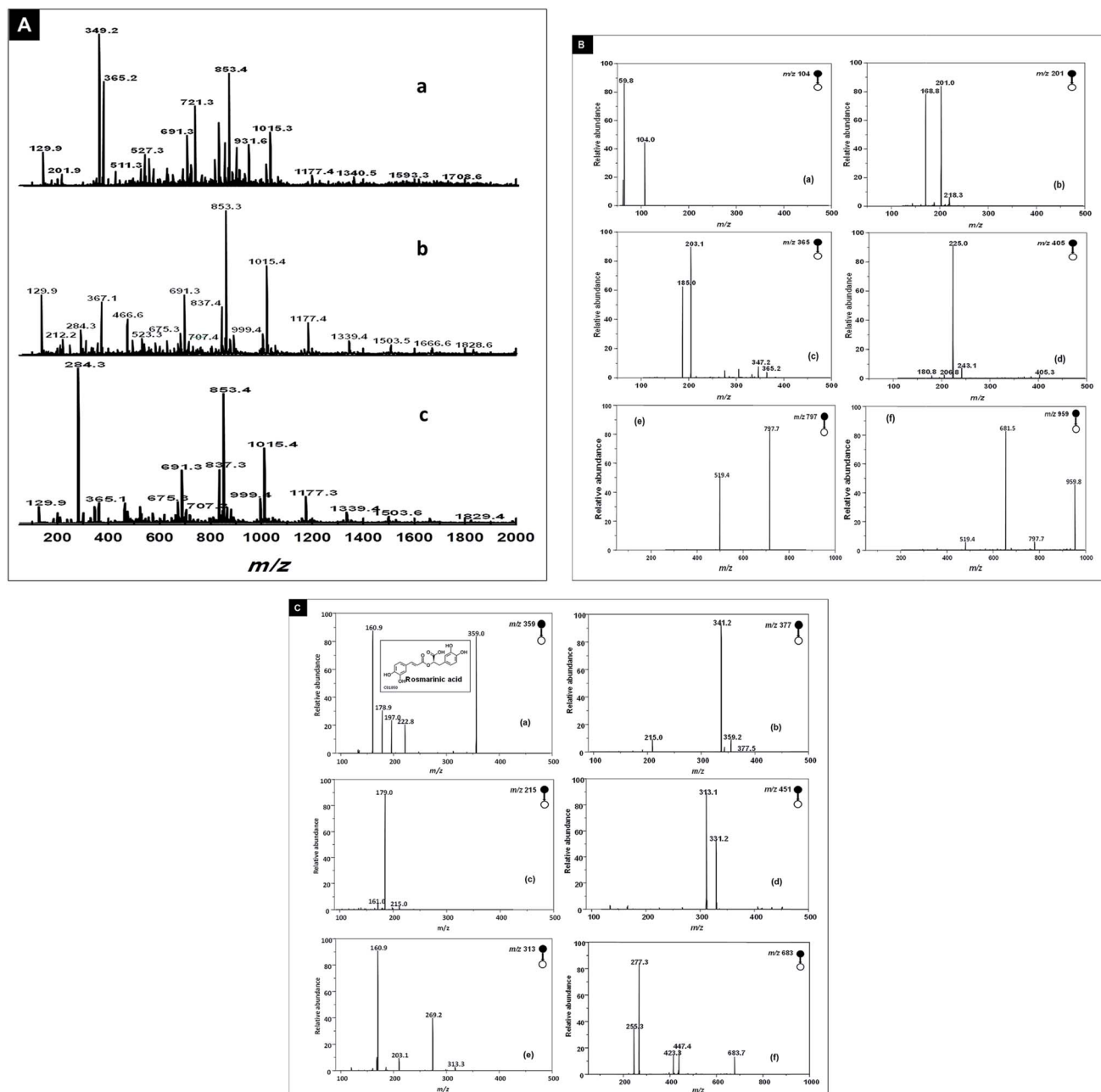


Fig. 3 ESI MS mass spectra (A) showing differences in metabolite profile of the leaf of *O. gratissimum* due to solvents (a-methanol, b-acetonitrile and c-chloroform). ESI MS-tandem mass spectra for selected metabolite ion peaks of leaf of *O. basilicum* in positive (B) and negative (C) ionization mode.

Illustrations with *O. gratissimum* show the differences in the metabolite profiles between DESI MS of leaf imprint (Fig. 2C) and ESI MS from leaf extract (Fig. 3A(a-c)). Besides, there were differences between the metabolite profile of TLC-imprint (Fig. 2A) and that of a direct leaf tissue (Fig. 2B). As reported with barley leaf,^{3b} the detached leaves of basil became dry and deformed quickly; hence, imprint imaging was followed for the study.

The metabolite distribution can be acquired in positive and negative ionization modes, as illustrated with *O. basilicum* (Fig. 1A and C). Tandem mass spectral imaging was done on respective ionization modes to get the fragmentation pattern for

identification of the predominant metabolite ion peaks. Few examples are shown in Fig. 3B and C. Elaborate details for finding metabolite adducts and matching tandem mass spectral data using database search is given in our previous report.¹⁹ For this study, the data acquired were also analyzed using MZmine software,²⁰ which has various processing algorithms for peak picking, base line correction *etc.* Peak lists were created and searched against the online databases. Different biomolecules tentatively identified by MZmine in this study include several terpene alcohols, fatty acids, phenolic and flavonoid glycosides *etc.* Literature abunds with gas or liquid chromatography based

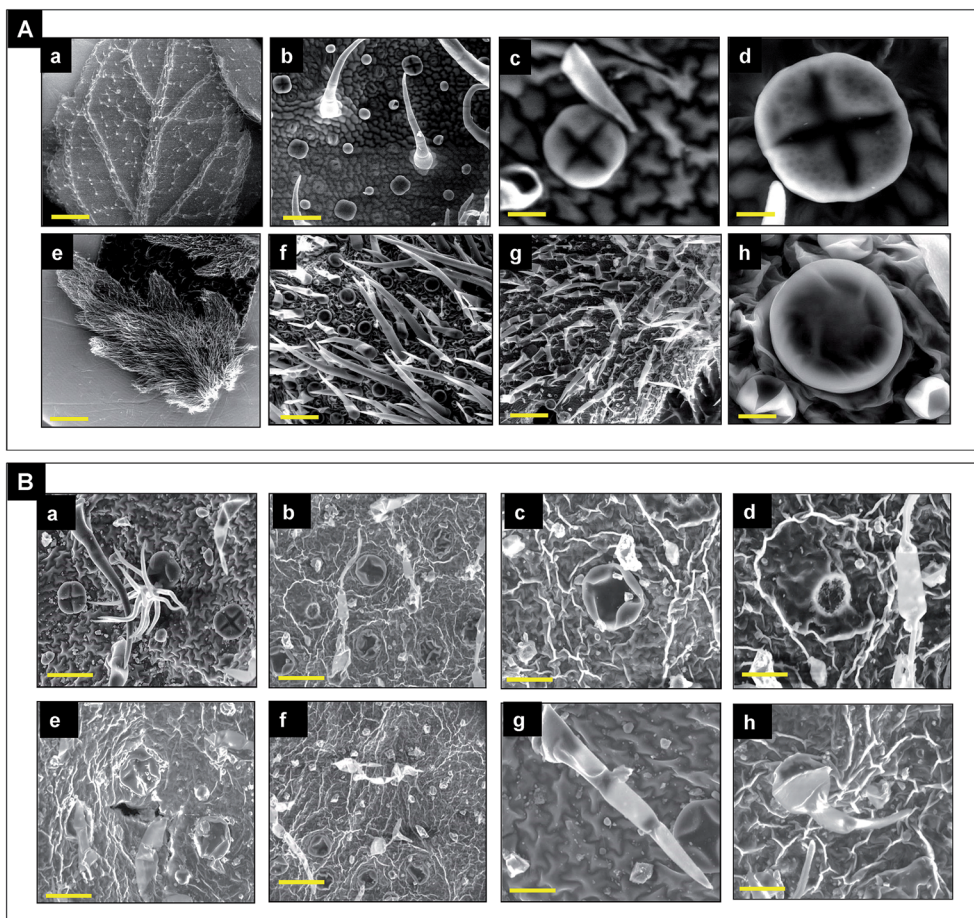


Fig. 4 Scanning electron micrographs of (A) healthy leaf of basil (a–d) and patchouli (e–h) showing trichomes and peltate glands at different magnifications. (B) *Fusarium* infected leaf showing the disease affected peltate gland and trichomes (a–h). The scale for images a and e are 500 μm and other images are 20–100 μm.

mass spectrometric (MS) methods on various bioactive molecules (essential oils, phenolic compounds, flavonoids, *etc.*) in different basil species with their tandem mass spectral data.²⁶ Most of the studies to date on basil have tabulated information on both positive and negative ions of phenolics, flavonoids and essential oils, *etc.*²⁷ So far, preferential detection/extraction of such bioactive compounds have specific requirements of suitable solvents and other instrumental parameters; if those parameters are adapted it is easy to identify the spatial distribution of any targeted metabolite.

As reported,^{26,27} different phenolic compounds were detected in negative ionization mode; here (a) in Fig. 3C shows the fragmentation data for the predominant metabolite peak at m/z 359 in negative ion mode (Fig. 1B), which was identified as rosmarinic acid when the data were analyzed using search tool of databases. Likewise, several metabolites of different pathways (like phenylpropanoid, terpenoids, flavonoids, lipids and fatty acids *etc.*) were identified in this study. Examples are isoeugenol (m/z 165), caffeoyl alcohol (m/z 167), gallic acid (m/z 169), caffeic acid (m/z 179), ferulic acid (m/z 193), syringic acid (m/z 197), 5-hydroxy coniferyl alcohol (m/z 197), quercetin (m/z 301), *etc.* Here, the method highlights a possibility to identify the diversity of compounds as untargeted metabolite profiles

comprising of various classes of small molecular metabolites, without the need for internal standards. There are various factors such as growth stages, seasonal variation, irrigation water, drying, and storage, *etc.*^{28–30} and even, the position of leaf within the same plant could vary in the chemical composition.³¹ It is always difficult to identify and understand transient changes of the eluted metabolite peaks. Here we show that DESI MS imaging gives a snapshot of the transient changes due to the environment stress or any physiological factors.

Conventional identification of *Fusarium* wilt at the field level is time consuming since it involves the accumulation of the pathogen to a sufficient level that can produce visible symptoms. External manifestation of wilt disease as chlorotic leaves, drying leaf tips and stunted growth of plants, wilting of shoots, *etc.*, may overlap with water stress or other diseases. Though wilt disease in basil and patchouli display similar morphological features, wilt in patchouli is caused by *F. solani*.³² Visual differences between healthy and infected leaves are obvious only in advanced stages of infection. Confocal microscopy and thermal imaging^{33,34} were used to image the growth of *Fusarium* pathogen. Scanning electron microscope was used for this study, to observe the changes in the peltate glands and trichomes of both basil and patchouli leaves, as shown in Fig. 4A(a–f).

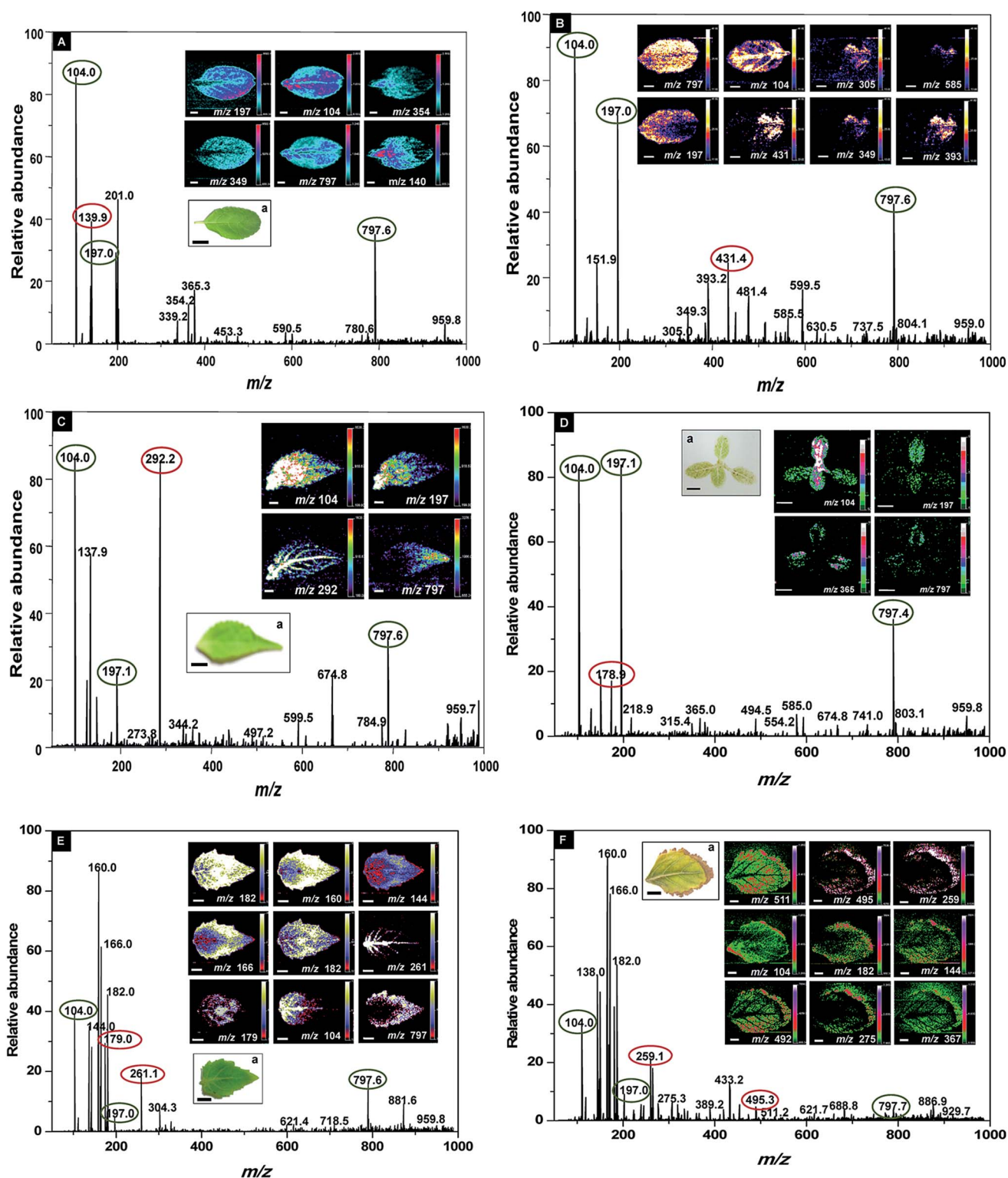


Fig. 5 DESI MS spectra and images showing the changes in predominant metabolites due to *Fusarium* infection in apparently healthy, asymptomatic (A) young leaf, (B) mature leaf of *O. basilicum*, (C) young leaf of *O. gratissimum*, (D) seedling of *O. basilicum* at four leaved stage, (E) asymptomatic young leaf of *P. cablin* and (F) mature leaf of *P. cablin* with visible symptom. Inset (a) in A, C and E shows the photograph of the apparent healthy young leaves used for DESI MS imaging. Inset (a) in D shows the upper surface of TLC-imprint of four leaved seedling of basil. Inset (a) in F is the upper surface of infected leaf showing brown discoloration on the margins. The scale is uniform in all the images (5 mm). The major peaks showing differences in spatial distribution are highlighted in the spectra with black and the fungal toxic metabolite peaks are highlighted with red circles.

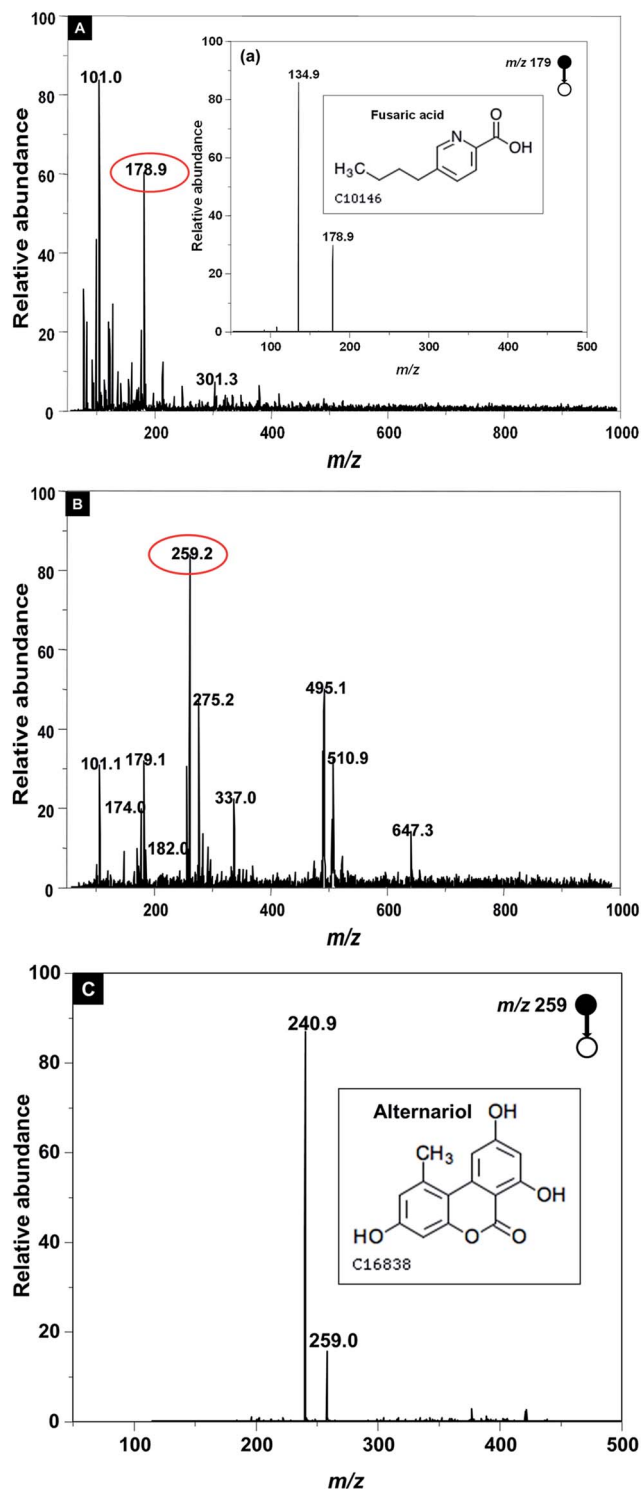


Fig. 6 DESI MS spectrum showing the toxic metabolites due to *Fusarium* (A) *Alternaria* (B) infection; spectrum extracted after subtraction of predominant metabolites peaks of apparently healthy, asymptomatic leaf of *O. basilicum* and *P. cablin*. Insets (a) and (c) show the fragmentation patterns of fusaric acid (m/z 179) and alternariol (m/z 259) respectively.

Both patchouli and basil species have many common features and in particular, terpenoids and phenylpropanoids compounds are reported to be stored in the peltate glands found on the leaf

epidermis.³⁵ The variations in the metabolite profile of basil and patchouli may be due to diversities in the terpenes and phenylpropanoids and the substrate specificity of different enzymes contribute to the production of complex blend of oxygenated linalool derivatives.^{36,37} As shown in (e) of Fig. 4A, young leaf of patchouli has trichomes in high density. During pathogen infection (Fig. 4B), there were necrotic spots in the trichomes and the peltate glands seem to have dilated. It is not feasible to use electron microscope for large scale screening purpose.

The challenge is that apparently healthy leaves that are asymptomatic carriers of the disease have to be identified by accurate, reliable and rapid detection methods. Hence both mature and young leaves showing no visible symptoms were selected for imaging, to identify the *Fusarium* contamination. Illustrations with clove basil given in Fig. 2C and D show that there is slight difference in metabolite profiles of young *versus* mature leaf of healthy plants. Small, apical leaves have a higher density of glands and trichomes (Fig. 4A). Small leaved varieties were reported to be susceptible to the disease.¹⁴ Hence, small, apical leaves with no visible symptoms (insets 'a' of Fig. 5A) were imaged in all selected plants. Typical plant metabolites that could serve as markers are given as DESI MS images (Fig. 5A–C).

Fig. 5B show the DESI MS images of *Fusarium* infected asymptomatic mature leaf of *O. basilicum*. Comparison of young *versus* mature infected basil leaf (Fig. 5A and B) show that a few metabolite ions (m/z 104, 197, 797, etc.) were present in both. Subtraction of metabolite peaks of healthy *versus* contaminated leaf of basil clearly indicated the presence of few metabolites including a metabolite peak at m/z 179, as shown in Fig. 6A. Tandem mass spectrometry along with database search was done and the ion peak at m/z 179 was identified as fusaric acid,³⁸ the primary toxic metabolite of any *Fusarium* pathogenic species. Hence the identification of such characteristic toxic metabolite peaks and their images can delineate the healthy leaf from the contaminated ones. All the three species varied in their responses to *Fusarium*. Spectra of *O. gratissimum* exhibited several other ions assignable to *Fusarium* (m/z 292) besides that corresponding to fusaric acid (m/z 179). In contrast, *O. tenuiflorum* DESI MS spectra did not display any ion corresponding to a known *Fusarium* metabolite. The intensity and spatial distribution of some metabolite ion peaks of the plant also got changed during pathogen infection as observed in all the three *Ocimum* species (Fig. 5A–D). There is species-specific responses to *Fusarium* infection, but several metabolites being common to all the three basil species (like m/z 104, 197, 797), were observed. Several metabolites and genes common in phenylpropanoid pathway is reported in basil or other species of Lamiaceae^{35,36} and the expression of few genes get altered during *Fusarium* infection.^{39a} Changes at germination or seedling stage due to *Fusarium* infection also reported.^{39b} Since the small sized basil seeds and even hydroponically grown basil also bear the *Fusarium* pathogen,¹³ the emerging seedling may contain the symptom; hence, growing seedlings of basil (Fig. S1C†) at four leaved stage was imaged. Fig. 5D shows the spectrum and DESI MS images for the four leaved seedling highlighting the reliability of the imaging method to screen plant leaves collected at any development stage.

The feasibility of extending this protocol to other related plant species/disease is also verified (Fig. 5E and F). In particular, very specific visible symptoms like brown, dried edges on leaf margin often overlap with nutrient stress and/or pathogenic infections. Fig. 5E shows the spectrum and images of an asymptomatic young leaf of patchouli. A mature leaf of patchouli with such visible symptom of brown, dry patches on the leaf margin is imaged and the results are given in Fig. 5F. As shown in inset 'a' of Fig. 5F, the corresponding DESI MS images (Fig. 5F) are very specific in locating the spot of infection. On comparing the contaminated leaf of patchouli (both Fig. 5E and F), with metabolite profile of healthy leaf (Fig. 2C), the predominant metabolite peaks (m/z 104, 144, 176, 182) and their DESI MS images were present in all. In Fig. 5F, DESI MS images of particular metabolite ions (m/z 259, 275, 495, 511) revealed the spatial location of the disease symptom, which were not visible in the TLC-imprint. Tandem mass spectrometry of metabolite ion m/z 259 gave fragment ions at m/z 241, which is identified as alternariol with database search (Fig. 6C). Alternariol is the primary toxin produced by pathogenic fungal species *Alternaria*, and in particular, the occurrence of *Alternaria* infection in basil is reported.⁴⁰ As shown in Fig. 5F, though the intensities of the peaks at m/z 492, 367, 511 were below 10%, still they could be extracted by subtraction of spectra of healthy versus contaminated ones (Fig. 6B). This shows the possibility to image the molecules particularly induced at the site of infection/inter junction, which may be a fungal toxic metabolite or a phytoalexin. It is reported that reddish brown color in pathogen affected area of leaf may be due to flavonoid phytoalexin namely, 3-deoxyanthocyanidins.⁴¹

Comparison of metabolite profiles in contaminated leaves of all the selected plants showed the presence of either or both toxic metabolite peaks *viz.*, fusaric acid (m/z 179) and alternariol (m/z 259), though the presence of other toxic metabolites (like altenuene, altenusin, tenuazoic acid, fusarenone-x *etc.*) were also identified using literature and database search.⁴² ESI Table S1† shows the details on molecular weight, structure, database reference *etc.*, for some of these toxic metabolites. Tandem mass spectral imaging of few of them (m/z 197, 261, 291, 293, *etc.*) showing relationships with each other is given in ESI Fig. S3.† For some of them it was difficult to assign the relationships or do further MSⁿ, because the presence of these metabolites was observed in images but the mass spectral intensity of the peak was below 10% (Fig. 5F). The basic methods for statistical analysis like principal component analysis and log-ratio plot analysis of the healthy and *Fusarium* infected plant samples were done using MZmine software. We checked our results with and without applying statistics and other algorithms; the results on DESI MS imaging are voluminous. Only a few images which are relevant to detection of pathogen contamination are presented in this manuscript. Some of the peaks showing disease symptoms or the intermediate reactions were of very low intensity, though their DESI MS images existed; hence the results given here are without any statistics and background correction. For this study, though we identified some metabolites we did not quantify them because there are no synthetic standard available for different

intermediate and interaction metabolites produced in the leaves during plant pathogen interactions. Hence the results shown here are pertaining only to the qualitative description; additional experiments are required to identify the specific *Fusarium* isolates and *Fusarium*-induced metabolite changes. But for rapid detection, it is relevant to check the presence of fusaric acid (m/z 179) and alternariol (m/z 259).^{38,40} These two metabolites are the principal toxic metabolites of *Fusarium* and *Alternaria*, from which other toxic metabolite ions are produced based on the local environment of the plant or pathogen. Hence, this method of DESI MS imaging is a rapid way to screen the leaves and can be interpreted even by nontechnical persons.

As observed in this study, several fungal metabolites including fusaric acid (m/z 179) and alternariol (m/z 259), are normally detected in positive ionization mode. Mass spectrometry is routinely used for the identification of different mycotoxins (the secondary metabolites produced by *Fusarium* fungi) in food and feed, that causes mycotoxicosis in humans and animals upon ingestion or inhalation.⁴² But it is challenging to determine which metabolite(s) may be responsible for the interaction or infection in plants, under natural growth conditions. Studies show that different metabolic pathways (like pectin, phenylpropanoid and carotenoid) get altered, and various signaling molecules like salicylic acid, methyl jasmonates and peroxidase enzymes are reported as inducing resistance to *Fusarium* in various plants.^{43,44}

Isolation of *Fusarium* species or its toxin(s) from the infected leaf was not attempted in this study, because it is reported that species of *Fusarium* which is nonpathogenic in one plant species may be pathogenic to other.⁴⁵ Besides, different strains or formae species of *Fusarium oxysporum* cannot be distinguished reliably in culture.⁴⁶ Even under controlled experimental conditions, with the inoculation of known strains of the pathogens in barley,⁴⁷ there were differences in the metabolites (like cinnamic acid, sinapoyl alcohol, coniferin, catechin and naringin) induced by trichothecene producing strain and its trichothecene non-producing mutant, thereby differentially regulating defense pathways associated with different resistant levels. In that context, for rapid detection we focused on toxic metabolite ions rather than looking for up/down regulated plant metabolites. Also, *Fusarium* wilt pathogen is reported to produce both toxic and nontoxic metabolites. The levels of contamination of banana fruits with *Fusarium oxysporum* f.sp. *ubense* (Foc) were reported to be too low, to be of concern to humans but appeared to contribute to the pathogenicity of the fungus during infection of banana plants.⁴⁸ For identifying several hundred cytotoxic fungal secondary metabolites, databases are available with details of full-scan high-resolution mass spectra and MS/MS spectra of both positive and negative ions.⁴⁹ Hence, the results illustrated with basil and patchouli suggests that this method may be the most suitable one for rapid screening for the disease, to find the toxic metabolites or the interaction of the *Fusarium* pathogen with any plant. Secondary metabolite biosynthetic genes responsible for the interaction of the *Fusarium* pathogen with of the host plant is decoded⁵⁰ and *Fusarium* genomics database is available.⁶ But intricate compositions of plant genetic, transcriptional and

epigenetic regulation appear to be a possible contributor to susceptibility or resistance to *Fusarium*.

The variations in chemical composition due to the polyploidy and outcrossing nature of the *Ocimum* species posed a great challenge. Hence, for the entire study period, periodically a number of leaf samples were imaged and the results stored as spectra and images for further reference. As there is limited knowledge on the metabolites involved in basil–*Fusarium*–environment interactions, this digitization helped to make comparison between different basil species or find out variations due to seasons on them. Other than the characteristic toxic metabolites of *Fusarium* and/or *Alternaria* species, the changes in the spatial distribution of selected metabolites in all selected plant species were identified in this manuscript. Besides, the identification of species-specific predominant metabolites demonstrated in this study with basil and patchouli strengthens the importance of DESI MS in rapid identification of authentic plant species. Results given here illustrate that it is a simple method suitable for any laboratory condition. However, the mass spectral and DESI MS data that are presented here are comparable, only when similar conditions are used for imaging. As Fob has host, climatic and regional preferences, there are chances for deviations from these results and number of chemical compounds which were present under our field conditions may vary elsewhere in all the three *Ocimum* species. The information and the methodology provided here may be applied precisely to any other crop species but instrumentation and solvent choices must always be tailored to the user defined circumstances and individual diagnostic situations. Handling large number of samples is possible as DESI MS has been successfully integrated into surgery for identification of tumor margins.⁵¹ Hence the methodology adapted here provides a valuable experimental system to address questions of agriculture and quarantine requirements.

Conclusions

Three different basil species (*O. gratissimum*, *O. basilicum* and *O. tenuiflorum*) were screened for *Fusarium* wilt by DESI MS imaging using TLC- imprints of leaves. Data were acquired in both positive and negative ionization modes to get information on predominant metabolite peak(s). The possibility to identify metabolite profile of the healthy plant(s) and compare it with that of the contaminated ones is illustrated with suitable examples. The changes represented in the spatial distribution of selected metabolites served as markers. Identification of toxic metabolites of *Fusarium* is illustrated with examples. The suitability of the method to screen *Fusarium* or other pathogen infection in related plant species is demonstrated using patchouli. The same instrument can be used for imaging the imprints or direct detection in tissues and/or measuring/quantification in extracts. The ease of interpretation of results by nontechnical persons will enable identification of contaminated plants and formulating effective control methods. Hence for rapid detection of contamination in any epidemics of *Fusarium*, DESI MS imaging would be ideal. This method of imaging will be highly useful in agriculture and in quarantine or

even in cases of disease outbreak, where there is urgency to screen large number of plant leaves.

Funding sources

Financial support is from the Department of Biotechnology (DBT) and Department of Science and Technology (DST), Government of India through the Nano Mission.

Conflict of interest

The authors declare no competing financial interest.

Acknowledgements

The authors thank the Department of Science and Technology, Government of India, for equipment support through the Nano Mission.

References

- 1 A. K. Jarmusch and R. G. Cooks, *Nat. Prod. Rep.*, 2014, **31**, 730–738.
- 2 C. Wu, A. L. Dill, L. S. Eberlin, R. G. Cooks and D. R. Ifa, *Mass Spectrom. Rev.*, 2013, **32**, 218–243.
- 3 (a) D. R. Ifa, A. Srimany, L. S. Eberlin, H. R. Naik, V. Bhat, R. G. Cooks and T. Pradeep, *Anal. Methods*, 2011, **3**, 1910–1912; (b) B. Li, N. Bjarnholt, S. H. Hansen and C. Janfelt, *J. Mass Spectrom.*, 2011, **46**, 1241–1246; (c) J. I. Zhang, X. Li, Z. Ouyang and R. G. Cooks, *Analyst*, 2012, **137**, 3091–3098.
- 4 J. Watrous, P. Roach, B. Heath, T. Alexandrov, J. Laskin and P. C. Dorrestein, *Anal. Chem.*, 2013, **85**, 10385–10391.
- 5 K. Chingin, J. Liang and H. Chen, *RSC Adv.*, 2014, **4**, 5768–5781.
- 6 L.-J. Ma, H. C. Van der Does, K. A. Borkovich, J. J. Coleman, M.-J. Daboussi, A. Di Pietro, M. Dufresne, M. Freitag, M. Grabherr, B. Henrissat, P. M. Houterman, S. Kang, W.-B. Shim, C. Woloshuk, X. Xie, J.-R. Xu, J. Antoniwi, S. E. Baker, B. H. Bluhm, A. Breakspear, D. W. Brown, R. A. E. Butchko, S. Chapman, R. Coulson, P. M. Coutinho, E. G. J. Danchin, A. Diener, L. R. Gale, D. M. Gardiner, S. Goff, K. E. Hammond-Kosack, K. Hilburn, A. Hua-Van, W. Jonkers, K. Kazan, C. D. Kodira, M. Koehrsen, L. Kumar, Y.-H. Lee, L. Li, J. M. Manners, D. Miranda-Saavedra, M. Mukherjee, G. Park, J. Park, S.-Y. Park, R. H. Proctor, A. Regev, M. C. Ruiz-Roldan, D. Sain, S. Sakthikumar, S. Sykes, D. C. Schwartz, B. G. Turgeon, I. Wapinski, O. Yoder, S. Young, Q. Zeng, S. Zhou, J. Galagan, C. A. Cuomo, H. C. Kistler and M. Rep, *Nature*, 2010, **464**, 367–373.
- 7 R. Hiltunen and Y. Holm, *Basil: The Genus Ocimum*, Taylor & Francis, 2003.
- 8 R. S. Verma, R. C. Padalia, A. Chauhan and S. T. Thul, *Ind. Crops Prod.*, 2013, **45**, 7–19.
- 9 (a) R. M. Davis, K. D. Marshall and J. Valencia, *Plant Dis.*, 1993, **77**, 537–537; (b) L. E. Datnoff, L. Z. Liang and R. L. Wick, *Plant Dis.*, 1997, **81**, 1214–1214; (c) L. Swart and J. M. Van Niekerk, *Australas. Plant Pathol.*, 2003, **32**, 125–126.

- 10 A. P. Keinath, *Plant Dis.*, 1994, **78**, 1211–1215.
- 11 A. M. Al-Hatmi, A. Bonifaz, G. de Hoog, L. Vazquez-Maya, K. Garcia-Carmona, J. F. Meis and A. D. Van Diepeningen, *BMC Infect. Dis.*, 2014, **14**, 588.
- 12 J. Evans, D. Levesque, A. de Lahunta and H. E. Jensen, *Vet. Pathol.*, 2004, **41**, 510–514.
- 13 (a) A. Chiocchetti, S. Ghignone, A. Minuto, M. L. Gullino, A. Garibaldi and Q. Migheli, *Plant Dis.*, 1999, **83**, 576–581; (b) A. Chiocchetti, L. Sciaudone, F. Durando, A. Garibaldi and Q. Migheli, *Plant Dis.*, 2001, **85**, 607–611; (c) M. Pasquali, P. Piatti, M. L. Gullino and A. Garibaldi, *J. Phytopathol.*, 2006, **154**, 632–636.
- 14 A. Reis, L. S. Boiteux and R. F. Vieira, *J. Gen. Plant Pathol.*, 2008, **74**, 375–381.
- 15 D. Chaimovitsh, N. Dudai, E. Putievsky and A. Ashri, *Plant Dis.*, 2006, **90**, 58–60.
- 16 F. Garcia-Bastidas, N. Ordonz, J. Konkol, M. Al-Qasim, Z. Naser, M. Abdelwali, N. Salem, C. Waalwijk, R. C. Ploetz and G. H. J. Kema, *Plant Dis.*, 2014, **98**, 694.
- 17 A. Gamliel, T. Katan, H. Yunis and J. Katan, *Phytopathology*, 1996, **86**, 56–62.
- 18 S. Veillet, V. Tomao and F. Chemat, *Food Chem.*, 2010, **123**, 905–911.
- 19 R. G. Hemalatha and T. Pradeep, *J. Agric. Food Chem.*, 2013, **61**, 7477–7487.
- 20 T. Pluskal, S. Castillo, A. Villar-Briones and M. Oresic, *BMC Bioinf.*, 2010, **11**, 395.
- 21 P. R. N. Vieira, S. M. de Moraes, F. H. Q. Bezerra, P. A. Travassos Ferreira, I. R. Oliveira and M. G. V. Silva, *Ind. Crops Prod.*, 2014, **55**, 267–271.
- 22 X. Zhang, H. Zhang, J. Pu, Y. Qi, Q. Yu, Y. Xie and J. Peng, *PLoS One*, 2014, **8**, e82841.
- 23 (a) K. Carovic-Stanko, A. Salinovic, M. Grdisa, Z. Liber, I. Kolak and Z. Satovic, *Plant Biosyst.*, 2011, **145**, 298–305; (b) M. Aghaei, R. Darvishzadeh and A. Hassani, *Rev. Cienc. Agron.*, 2012, **43**, 312–320.
- 24 S. Rastogi, S. Meena, A. Bhattacharya, S. Ghosh, R. K. Shukla, N. S. Sangwan, R. K. Lal, M. M. Gupta, U. C. Lavania, V. Gupta, D. A. Nagegowda and A. K. Shasany, *BMC Genomics*, 2014, **15**, 588.
- 25 A. K. Badu-Tawiah, L. S. Eberlin, Z. Ouyang and R. G. Cooks, *Annu. Rev. Phys. Chem.*, 2013, **64**, 481–505.
- 26 Z. Wang, P. Chen, L. Yu and P. D. B. Harrington, *Anal. Chem.*, 2013, **85**, 2945–2953.
- 27 C. Jayasinghe, N. Gotoh, T. Aoki and S. Wada, *J. Agric. Food Chem.*, 2003, **51**, 4442–4449.
- 28 A. I. Hussain, F. Anwar, S. T. Hussain Sherazi and R. Przybylski, *Food Chem.*, 2008, **108**, 986–995.
- 29 S. Ekren, C. Sonmez, E. Ozcakal, Y. S. K. Kurttas, E. Bayram and H. Gurgulu, *Agr. Water Manag.*, 2012, **109**, 155–161.
- 30 (a) D. Sarkar, A. Srimany and T. Pradeep, *Analyst*, 2012, **137**, 4559–4563; (b) A. Ghasemi Pirbalouti, E. Mahdad and L. Craker, *Food Chem.*, 2013, **141**, 2440–2449.
- 31 R. Fischer, N. Nitzan, D. Chaimovitsh, B. Rubin and N. Dudai, *J. Agric. Food Chem.*, 2011, **59**, 4913–4922.
- 32 S. S. Chavan and S. K. Prashanthi, *Indian Phytopathol.*, 2011, **64**, 258–260.
- 33 A. Bolwerk, A. L. Lagopodi, B. J. Lugtenberg and G. V. Bloemberg, *Mol. Plant-Microbe Interact.*, 2005, **18**, 710–721.
- 34 K. J. Czymmek, M. Fogg, D. H. Powell, J. Sweigard, S.-Y. Park and S. Kang, *Fungal Genet. Biol.*, 2007, **44**, 1011–1023.
- 35 Y. Iijima, R. Davidovich-Rikanati, E. Fridman, D. R. Gang, E. Bar, E. Lewinsohn and E. Pichersky, *Plant Physiol.*, 2004, **136**, 3724–3736.
- 36 F. Deguerry, L. Pastore, S. Wu, A. Clark, J. Chappell and M. Schalk, *Arch. Biochem. Biophys.*, 2006, **454**, 123–136.
- 37 C. Deschamps and J. E. Simon, in *Plant Secondary Metabolism Engineering*, Springer, 2010, pp. 263–273.
- 38 (a) X. Dong, N. Ling, M. Wang, Q. Shen and S. Guo, *Plant Physiol. Biochem.*, 2012, **60**, 171–179; (b) X. Dong, Y. Xiong, N. Ling, Q. Shen and S. Guo, *World J. Microbiol. Biotechnol.*, 2014, **30**, 1399–1408.
- 39 (a) K. Kostyn, M. Czemplik, A. Kulma, M. Bortniczuk, J. Skala and J. Szopa, *Plant Sci.*, 2012, **190**, 103–115; (b) I. Morkunas, M. Stobiecki, L. Marczak, J. Stachowiak, D. Narozna and D. Remlein-Starosta, *Physiol. Mol. Plant Pathol.*, 2010, **75**, 46–55.
- 40 (a) A. H. Aly, R. Edrada-Ebel, I. D. Indriani, V. Wray, W. E. G. Muller, F. Totzke, U. Zirrgiebel, C. Schachtele, M. H. G. Kubbutat and W. H. Lin, *J. Nat. Prod.*, 2008, **71**, 972–980; (b) G. Gilardi, M. L. Gullino and A. Garibaldi, *J. Plant Pathol.*, 2013, **95**, 41–47.
- 41 A. Poloni and J. Schirawski, *Molecules*, 2014, **19**, 9114–9133.
- 42 (a) M. Marchetti-Deschmann, W. Winkler, H. Dong, H. Lohninger, C. P. Kubicek and G. Allmaier, *Food Technol. Biotechnol.*, 2012, **50**, 334–342; (b) P. M. Scott, W. Zhao, S. Feng and B. P. Y. Lau, *Mycotoxin Res.*, 2012, **28**, 261–266.
- 43 (a) W. Wojtasik, A. Kulma, K. Kostyn and J. Szopa, *Plant Physiol. Biochem.*, 2011, **49**, 862–872; (b) A. Boba, A. Kulma, K. Kostyn, M. Starzycki, E. Starzycka and J. Szopa, *Physiol. Mol. Plant Pathol.*, 2012, **76**, 39–47.
- 44 (a) Z. Wang, C. Jia, J. Li, S. Huang, B. Xu and Z. Jin, *Funct. Integr. Genomics*, 2014, 1–16; (b) H. D. Ardila, A. M. Torres, S. T. Martinez and B. L. Higuera, *Physiol. Mol. Plant Pathol.*, 2014, **85**, 42–52.
- 45 T. Kashiwa, K. Inami, M. Fujinaga, H. Ogiso, T. Yoshida, T. Teraoka and T. Arie, *J. Gen. Plant Pathol.*, 2013, **79**, 412–421.
- 46 J. F. Leslie and B. A. Summerell, *The Fusarium Laboratory Manual*, Wiley Online Library, 2007.
- 47 G. K. Kumaraswamy, A. C. Kushalappa, T. M. Choo, Y. Dion and S. Rioux, *Plant Pathol.*, 2012, **61**, 509–521.
- 48 C. Li, C. Zuo, G. Deng, R. Kuang, Q. Yang, C. Hu, O. Sheng, S. Zhang, L. Ma and Y. Wei, *PLoS One*, 2013, **8**, e70226.
- 49 T. El-Elimat, M. Figueroa, B. M. Ehrmann, N. B. Cech, C. J. Pearce and N. H. Oberlies, *J. Nat. Prod.*, 2013, **76**, 1709–1716.
- 50 (a) D. W. Brown, R. A. E. Butchko, M. Busman and R. H. Proctor, *Fungal Genet. Biol.*, 2012, **49**, 521–532; (b) D. W. Brown, R. A. Butchko, S. E. Baker and R. H. Proctor, *Fungal Biol.*, 2012, **116**, 318–331.
- 51 K. S. Kerian, A. K. Jarmusch, V. Pirro, M. O. Koch, T. A. Masterson, L. Cheng and R. G. Cooks, *Analyst*, 2014, **140**, 1090–1098.